IEEJ International Workshop on Sensing, Actuation, Motion Control, and Optimization

System Integration and Control of Mechatronic Imaging Systems

E. Csencsics*a) Non-member, S. Ito* Non-member
J. Schlarp* Non-member, G. Schitter* Non-member

Mechatronic imaging systems, ranging from nanoscale manufacturing and metrology to telescope systems and adaptive optics for astronomy, are complex machines that demand a continuous improvement of system speed, range, and precision. This requires advanced mechatronic designs, sophisticated motion control, as well as a proper system integration in order to obtain the maximum performance of the resulting overall system. This paper discusses the interplay between process and control design, and presents the example for the system design, control and integration of a scanning laser system for precision 3D triangulation metrology.

Keywords:

1. Introduction

The high-tech industry requires in various applications mechatronic systems with extreme performance in precision and speed. Precision engineering is an important field of research for the continuous development of mechatronic imaging systems, such as atomic force microscopes (AFM) [1], wafer scanners [2], adaptive optics [3], and scanning laser metrology and microscopy [4] [5], in order to further improve the performance of these systems and machines.

What is common to all these applications is the combination of precision motion control, a high dynamic range of several orders of magnitude, and a well-timed and synchronized data acquisition and control system for recording the independent sensor information, in case of metrology applications [6] [7], or for manipulating the light, e.g. in projection systems [8].

Mechatronic imaging systems for future applications require even higher performance in terms of positioning bandwidth, actuation range, imaging speed, and precision. This can be achieved by advanced mechatronic designs and highly sophisticated motion control. Already at the system design phase all components involved in the specific application have to be considered, where a well predictable behavior of all system components is required [9]. Examples for these components are the mechanical structure of the positioning system, the power amplifier, the actuators, the sensors, electronics, and the real-time control system. A proper system integration, utilizing the interplay between process design and control design, allows optimizing the performance of the mechatronic imaging system for the specific application.

For nano-metrology applications, AFMs are a very important tool for imaging on the atomic and molecular level. However, the scanning based measurement in AFM is a limiting factor for the imaging speed of those systems. By improved mechatronic design and system integration the imaging speed of AFMs has been improved by three orders of magnitude [1], which includes a novel design of the AFM scanning unit [10] as well as modern control methods [11] [7].

In confocal laser scanning microscopy adaptive optics and improved motion control of the scanning mirrors enabled a significant improvement in imaging resolution [12] as well as a 70-fold reduction of the tracking error [4] when scanning at high speeds.

This paper presents the system design and integration of a laser triangulation 3D metrology system. Optical sensors play an increasingly important role in the automation of manufacturing and verification processes, due to high acquisition speeds, non-contact principles and therefore non-destructiveness, and simultaneous measurements in more than one dimension [13]. In addition, sub-micrometer accurate 3D measurement sensors become more and more important in the application of consumer products [14]. Although tactile and other non-optical metrology systems proved themselves successful over the last decades, they are progressively replaced for high precision applications by e.g. laser triangulation or chromatic confocal sensors [15].

2. Scanning Metrology Systems

The function of scanning metrology systems can be split into three main tasks. The first is providing the scanning motion in X- and Y-direction in order to enable the measurement of an area of interest instead of just a single point. The second is the actual metrology task for obtaining the spatially resolved sensor information. The third main task is the synchronized data acquisition for recording the metrology sensor information as a function of the position in the X-Y plane, encoding the metrology sensor data and forming a false-color image.

a) Correspondence to: csencsics@acin.tuwien.ac.at
* The authors are with the Christian Doppler Laboratory for Precision Engineering for Automated In-Line Metrology at the Automation and Control Institute, Technische Universitat Wien, A-1040 Vienna, Austria.

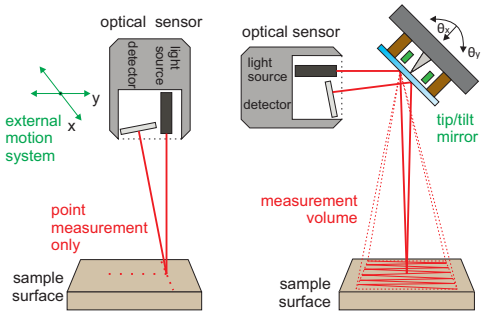

(a) Point measurement (b) Areal measurement

Fig. 1. Principle of integrating a triangulation sensor with a FSM system. Redirecting the optical path enables an advancement from (a) single point to (b) areal measurements.

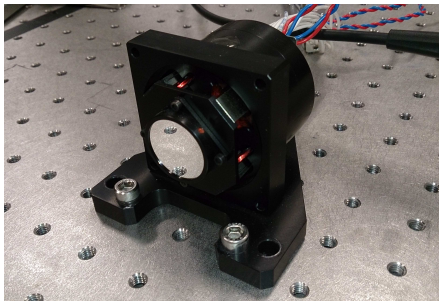

Fig. 2. State of the art fast steering mirror system from Optics in Motion. The 1" diameter mirror is actuated by two voice coils per axis and has a range of ± 26.2 mrad. The internal sensor system measures the mirror position in tip and tilt.

The task of scanning can be performed by moving the sample under test, which is common in some AFM designs [6], by moving the metrology sensor [16], or in case of optical metrology by scanning e.g. the laser [8].

The achievable resolution and imaging speed is, next to the fundamental limits of the actual metrology sensing principle, given by the achievable precision and bandwidth of the scanning unit. This is the most critical component, where mechatronic system design is vital [9]. For the actuation typically piezoelectric [10] or electromagnetic actuators [8] [9] are utilized, determining the achievable actuation force, and thus speed, as well as range of the scanning unit. In most scanning systems, the position is monitored by position sensors, which determine the achievable resolution. The proper integration of the actuators and sensors in the mechanical structure of the scanning unit determines the performance that can be achieved by the motion control system. The control itself can be performed in open-loop, for open-loop stable systems [6], closed-loop [8], two-degrees-of-freedom control [11], or by repetitive [17] and iterative-learning-based approaches [18] [4].

3. Scanning Optical 3D Metrology

In contrast to point-wise measuring scanning systems using a tactile probe, an optical metrology system does not have to be moved entirely to scan a sample. Instead the respective sensor system can remain stationary, while only the light path of the optical system is manipulated, which can be an enabler for improving measurement speeds, precision and versatility of optical metrology systems.

By integrating optical metrology sensors with opto-mechatronic components, e.g. fast steering mirrors (FSMs), as shown in Fig. 1(b), motion control and measurement algorithms for real-time data processing, a single point sensor, as shown in Fig. 1(a), could be advanced to a flexible 3D metrology tool [19]. Various imaging and manufacturing systems already incorporate a scanning laser or light beam. They are ranging from laser confocal sensor systems [20], confocal microscopy [5] and laser triangulation with fixed patterns [21] to selective laser melting or selective laser sintering in additive manufacturing processes [22] and laser welding processes [23]. Improving performance by an integrated approach requires customized solutions of the opto-mechatronic components since the target application has a significant influence on the scanner design and the mode of operation, as in the case of task optimized scan trajectories [24] [8].

FSM systems, as shown in Fig. 2 (Type: OIM102, Optics In Motion LLC, Long Beach, USA), are optomechatronic devices that enable tip and tilt motion (typically single degrees) of an attached mirror by a set of voice coil actuators and include internal sensors for position measurement and control. When using such a FSM to deflect a laser or light beam for the 2-dimensional scanning of an area of interest within a 3D optical scanning metrology system, motion control by means of feedback is inevitable to ensure a precise scanning motion and a high tracking performance in lateral direction. In the sense of an integrated system design, such feedback controllers should be tailored dependent on the pre-determined scanning motion in order to maximize the entire system performance.

3.1 Scanning Trajectories The most commonly used type for such a purpose is the raster trajectory [25] [26], which is also applied in numerous other scientific instruments, e.g. scanning probe microscopy [6]. For a triangular reference signal at least the first 7-11 harmonics of the fundamental frequency should be covered by the system bandwidth [27]. For this reason typically controllers enabling a high closed-loop bandwidths are required, which can impose stringent requirements on the mechanical design of the FSM [28].

An alternative are Lissajous trajectories, which have recently been proposed for precision scanning systems such as AFMs [29]. They result from driving each system axis with a sinusoidal signal of a fixed frequency, with the drive frequencies determining the spatial resolution and the frame rate [30]. The spatial resolution of a Lissajous scan is non-uniform, with the maximum distance between two intersections of the scan trajectory

Post-print version of the article: Ernst Csencsics, Shingo Ito, Johannes Schlarp and Georg Schitter, "System Integration and Control of Mechatronic Imaging Systems," *the 4th IEEJ International Workshop on Sensing, Actuation, Motion Control, and Optimization* , Tokio, Japan, 2018.

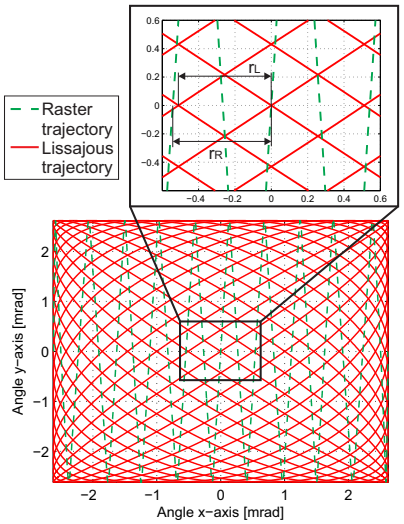

Fig. 3. Comparison of a raster (solid red) and a Lissajous trajectory (dashed green) for performing a 2-dimensional scan of an area. The fast axis of the raster scan is set to 10 Hz and the Lissajous frequencies are set to f_x =19 Hz and f_y =14 Hz, resulting in an equal frame rate and an almost equal spatial resolution r_R for the raster and r_L for the Lissajous scan (zoomed image) [24].

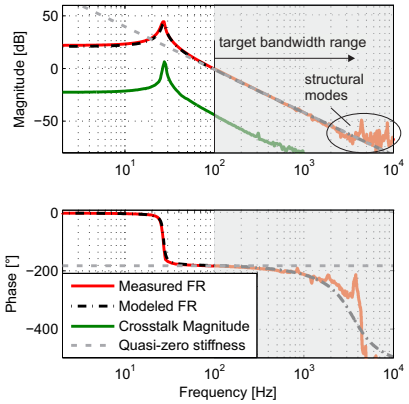

Fig. 4. Frequency response of a low stiffness FSM and a generic quasi-zero stiffness mechatronic system (dashed gray). The response of one FSM axis (solid red) is shown together with the fitted system model (dashed black) and the measured crosstalk (solid green) [24].

and the principle axes being a simple and efficient metric for it. The spatial resolution is building up gradually with evolving scan time, being termed multi-resolution, and may be a particularly valuable property for metrology systems in industrial applications. Fig. 3 shows a comparison of an exemplary raster and a Lissajous scan trajectory. With the chosen raster (10/0.5 Hz) and Lissajous frequencies (19/14 Hz), trajectories with almost equal spatial resolution at a rate of 1 frame/s are obtained.

3.2 PID Alpha Tuning A frequently used controller type, which is due to the wide control bandwidth perfectly suited for raster trajectories, is the PID controller [31]. In order to intuitively tune the gains in the face of the tradeoff between robustness (stability margins, parameter variation) and performance (response time, tracking performance), which are typically the important properties of the closed-loop system in practical applications, the loop shaping based *Alpha tuning method* for the design of PID controllers has been proposed [32], which is applicable low stiffness mechatronic systems that are showing a double integrator characteristic beyond the suspension mode and are typically controlled on their mass line (see gray area in Fig. 4). This system class includes many mechatronic positioning applications, ranging from wafer scanners [2] over CD player pickup heads to voice coil actuator based linear motion drives [33] and FSMs [24]. Fig. 4 depicts the frequency response of one axis of the low stiffness FSM in Fig. 2, shown together with its fitted model [24] and crosstalk response and a generic quasi-zero stiffness system response.

By using a suitable parametrization for the controller gains the *Alpha tuning method* reduces the number of design parameters to two: the open-loop cross-over frequency ω_c and a single tuning parameter α [32]. The cross-over frequency ω_c is usually either maximized for high performance, typically limited by structural modes of the positioned mass (beyond 3 kHz in Fig. 4), or fixed by the requirements of the respective application, e.g. the targeted trajectory in a scanning system. The tuning parameter α adjusts the spectral distance between the corner frequencies of the P-, I- and D-component that separate the control actions in the frequency domain and enables a direct tradeoff between performance and robustness of the closed-loop system [32]. An independent tuning of the controller gains is prevented, such that an overlapping and interference of control actions, mutually diminishing their desired action and the overall system performance, is avoided. Fig. 5 shows transfer functions (TFs) of controllers for the low stiffness FSM (see Fig. 4) for a target cross-over frequency $f_c = 400$ Hz and α-values of 2, 3, and 4.5. Higher α-values increase the phase margin and also the controller gain at high frequencies while decreasing the gain at low frequencies. This means that for large values of α the system becomes more robust, but the disturbance rejection and tracking performance at low frequencies is reduced due to the lower loop gain. The increased gain at higher frequencies additionally leads to an increased sensor noise feedback. Lower α-values have the inverse effects as they increase the performance at low frequencies and reduce the sensor noise feedback at the cost of a degraded robustness (lower phase margin). The value $\alpha = 3$ represents a good tradeoff between robustness (phase margin of 54°) and performance of the closed-loop controlled

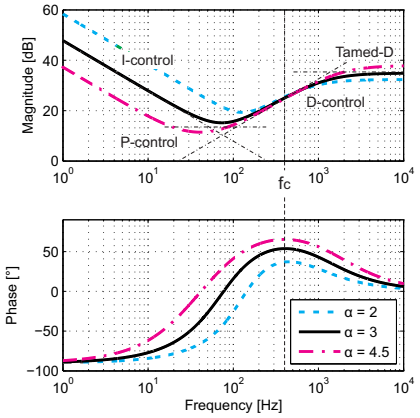

Fig. 5. Influence of the tuning parameter α on the TF of the resulting controller. The controllers for α-values of 2, 3 and 4.5 are shown [32].

low stiffness FSM system [32].

3.3 Dual Tone Control The required large control bandwidth for raster trajectories imposes strict requirements on the mechanical design of the FSM system [28], and the tracking errors even with the best performing PID controller are still significant, especially at the turning points of the triangle [34]. Lissajous trajectories can relax these design challenges and improve the tracking performance. Under the assumption that the control task is the precise tracking of a defined Lissajous trajectory and no disturbance rejection capability at low frequencies is required, it is possible to shape the single-input-single-output (SISO) feedback controller of each system axis to a single tone, with a high control gain localized at the sinusoidal drive frequency of the individual axis [29]. To also reject the small but present amount of inter-axis crosstalk in the system (see Fig. 4), dual tone (DT) controllers with a high controller gain localized around both driving frequencies have been proposed [24]. The controllers are obtained by H_∞ control synthesis [35], allowing the specification of requirements on the controller in a parametric way by using suitable weighting functions.

In Fig. 6(a) the TFs of the DT and a PID controller (designed for $\omega_c = 500$ Hz and $\alpha = 3$) are compared, showing with more than 45 dB significantly higher control gains of the DT controller at the Lissajous drive frequencies and lower gains at all other frequencies as compared to the PID controller. The complementary sensitivity functions for reference tracking of the resulting closed-loop systems are depicted in Fig. 6(b). The system with the PID controller has a control bandwidth of 730 Hz and is thus suitable for tracking a triangular reference signal of up to 100 Hz, with the first 7 harmonics covered. The PID controller can also be used for Lissajous trajectories with drive frequencies up to the control bandwidth. The system with the DT controller reaches the 0 dB line exactly at the two drive frequencies, while remaining below -40 dB at lower and higher frequency ranges. Employing a right half plane zero results in a perfect phase match of 360° and 720° at the drive frequencies.

Experiments show that the Lissajous scan (152/215 Hz) with the tailored DT controller results in a factor 40 smaller rms tracking error when compared to tracking the same Lissajous trajectory with the PID controller [24], which is explained by the mismatches in the phase and gain (peaking before the roll-off) at higher frequencies, as consequence of the PID design (see Fig. 6(b)). Comparing the conventional raster scan with the PID controller to the Lissajous scan with the DT controller, both trajectories having the same temporal and spatial resolution, shows a reduction of the tracking error by one order of magnitude. The rms current for actuation in the Lissajous/DT case is, however, significantly increased and above 2.3 times higher than for the raster/PID case, which limits the range of high-resolution Lissajous scans with higher drive frequencies. This is due to the higher fundamental frequencies of the Lissajous scan, which are required to obtain the same spatial resolution as the raster trajectory.

4. System Integration

An integrated controller design, considering the properties of the desired trajectory type and including them already in the design phase of the controller, enables a significant reduction of the tracking error. Extending the level of system integration from the trajectory and control design further to the

mechatronic system design of the FSM allows to mitigate limitations, such as the reduced range due to the high current consumption in the Lissajous case, and to further improve the system performance.

4.1 Resonant FSM The performance in terms of speed and range of a voice coil actuated FSM system (see Fig. 2), enabling a large angular range [36], is limited by the maximum actuator force, determined by the maximum permissible coil current. The first approach to relax this limitation can be to maximize the actuator's motor constant, but there will be a physical limit this actuation technology cannot exceed. Looking at the feedback control loop and its loop gain, as indicator for frequency ranges with good tracking performance, it can be seen that, if a certain loop gain is required at a defined frequency in order to result in a desired tracking performance, there is no difference how the loop gain is distributed over the plant and the controller. This means that the high controller gains of the DT controllers at the desired drive frequency, leading to high actuator currents, could also be redistributed to the plant gain of the FSM dynamics. Considering a system tailored for the continuous dynamic scan case, this can be achieved by retuning the resonance frequencies of the suspension mode for each axis to the desired drive frequency [8]. At the resonance the torque and angular velocity are in phase, such that the torque acts in

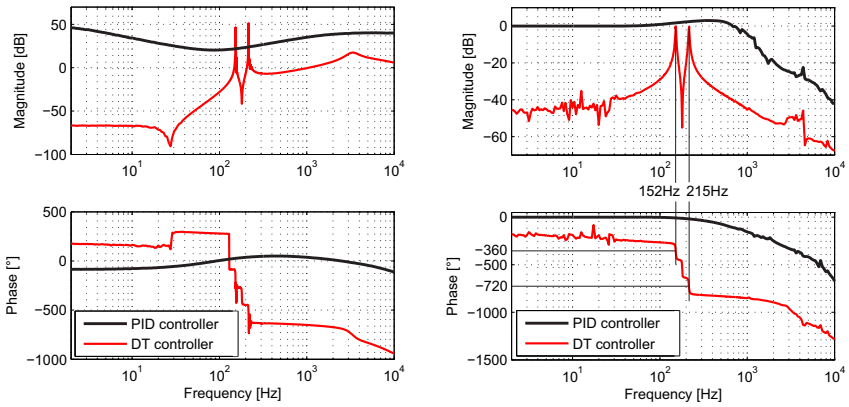

(a) Controller transfer functions (b) Complimentary sensitivity functions

Fig. 6. Comparison of the DT and PID controller. (a) shows the measured transfer functions of the implemented controllers. The DT controller shows high control efforts localized at both drive frequencies (152/215 Hz). (b) depicts the measured complimentary sensitivity function of the FSM for both controllers [24].

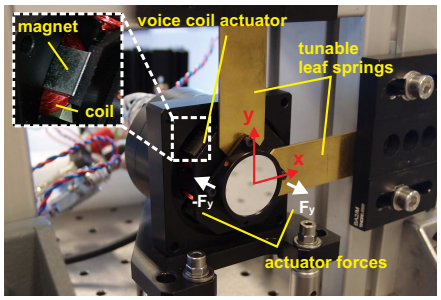

Fig. 7. Tuned FSM system. The spring constants of x- and y-axis are increased using tunable leaf springs. The resonance frequencies can be tuned by adjusting the length of each leaf spring [8].

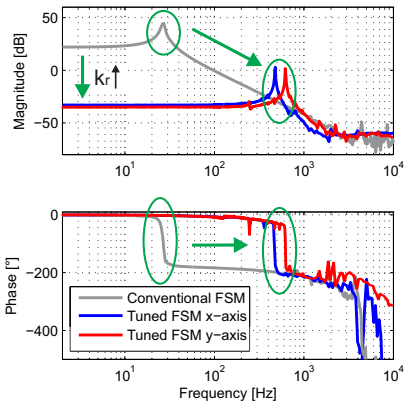

Fig. 8. Frequency responses of FSM systems. The frequency response of the tuned x- (blue) and y-axis (red) and the response of the conventional FSM system (gray) are shown. The resonance frequencies are shifted to $f_{0x} = 473$ Hz and $f_{0y} = 632$ Hz, respectively, and increase the plant gain by more than 30 dB [8].

the direction of the movement and thus maximizes the work [9]. By this approach the scanning motion of the FSM tracking the desired Lissajous trajectory can be performed with maximum efficiency.

The resonance frequency $\omega_0 = \sqrt{k_r/J}$ of a low stiffness FSM can be increased by either (i) reducing the system's inertia J, which lifts the mass line, or (ii) by increasing the rotational spring constant k_r of the guiding flexures, which lowers the spring line (see Fig. 8). An increase of the spring constant is easily feasible and a tunable mechanism that enables the adjustment of the exact resonance frequency can be attached to the existing system. Fig. 7 shows the setup of the tuned FSM with leaf springs of adjustable length to tune the resulting stiffness. The frequency response of the conventional FSM and the tuned FSM are depicted in Fig. 8. The resonance frequency of the x- and y-axis are tuned to $f_{0x} = 473$ Hz and $f_{0y} = 632$ Hz, respectively, by increasing the system stiffness by a factor of 512 and 630 as compared to the conventional FSM, resulting in a significantly higher plant gain at this frequency due to the low damping.

For comparison of the tuned and the conventional FSM, both systems are tracking the desired reference Lissajous trajectory with the related DT controllers, while increasing the scan amplitudes until the current limit of the actuator coils is reached. Fig. 9(a) depicts the current consumption of both FSM configurations and shows that the current consumption of the tuned FSM is 10 times smaller, denoting a reduction of dissipated energy in the coils by a factor of 100. Due to

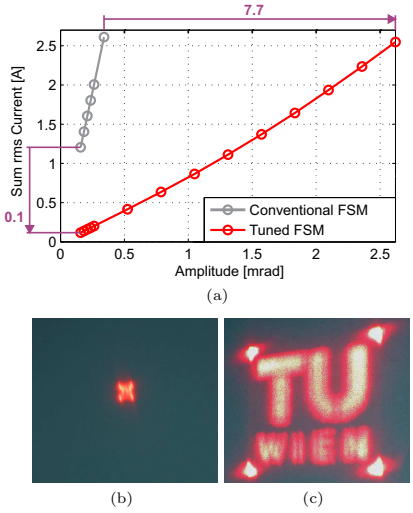

Fig. 9. Reduced current consumption and enlarged scan area. (a) compares the rms current for the conventional (black) and the tuned FSM system (red). (b) and (c) compare the images of a projection system using the conventional and the tuned FSM, respectively, to track the Lissajous reference at the respective maximum scan amplitude (0.34 mrad and 2.62 mrad) [8].

the reduced current consumption the tuned FSM also has a 7.7 times larger scan range, entailing an about 60 times larger scan area. In Fig. 9(b) and Fig. 9(c) the projected patterns of a laser projection system employing the conventional and the tuned FSM are shown, respectively, clearly illustrating the 60-fold increase in scan area when using the tuned FSM.

5. Application of 3D Optical Metrology

According to the concept shown in Fig. 1(b) the scanning optical sensor system, shown in Fig. 10, consists of a laser triangulation sensor (Type: ILD 2300-100, Micro-Epsilon GmbH, Germany), with a measurement range of 100 mm and the FSM from Fig. 2, for scanning the measurement point over the sample surface. To record a three dimensional image of the sample, both optical paths of the triangulation sensor are manipulated by the FSM. Since the transmission and the reflection path of the sensor are manipulated by the mirror, there is no difference from the perspective of the sensor whether the optical path is manipulated by the FSM or not [16]. Therefore, this setup satisfies the Scheimpflug condition which entails a sharp projection of the diffusely reflected laser point from the sample onto the detector. With the geometrical relations of the setup, the surface profile of a sample can be reconstructed from the sensor measurement and the angular position of the FSM [16], which simultaneously also removes the scanner bow. To correct for a tilted sample plane a RANSAC algorithm, which detects and subtracts a flat

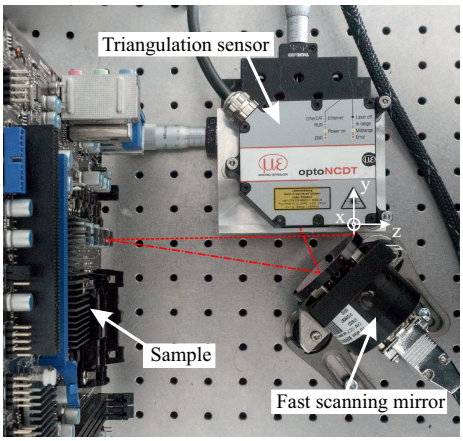

Fig. 10. Experimental setup of the scanning laser triangulation sensor. With a tip-tilt mirror the optical paths of the triangulation sensor are manipulated.

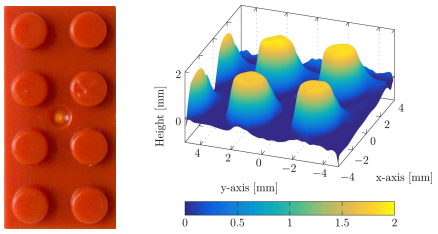

Fig. 11. 3D measurement results of the in (a) shown nano block which has a dimension of 16 x 8 x 2 mm. The in (b) depicted reconstructed surface profile shows good agreement with the sample.

surface, is used [37]. Lissajous-based scan trajectories with driving frequencies of $f_1 = 27$ Hz and $f_2 = 52$ Hz are applied to the metrology system to scan the sample, utilizing DT controllers for the scanning axes of the FSM [8]. The resulting measurement system has a scan area of 16 x 16 x 100 mm and provides resolutions of 900 x 900 x 30 μm for the respective x-, y- and z-axis. The image resolution can be further increased by detecting and rescanning areas with interesting features [38].

In Fig. 11 and Fig. 12 the measured sample surfaces of two samples, scanned with the Lissajous trajectory, are shown. In both cases the measurement results show good agreement with reference measurements obtained by a linearly scanned line sensor (data not shown).

In summary it is shown that the integrated mechatronic design of the FSM in combination with a laser triangulation sensor and an appropriate data acquisition system forms an integrated high performance optical 3D metrology system.

6. Conclusions

This paper demonstrates that considerable performance improvements of mechatronic imaging systems

Post-print version of the article: Ernst Csencsics, Shingo Ito, Johannes Schlarp and Georg Schitter, "System Integration and Control of Mechatronic Imaging Systems," *the 4th IEEJ International Workshop on Sensing, Actuation, Motion Control, and Optimization* , Tokio, Japan, 2018.

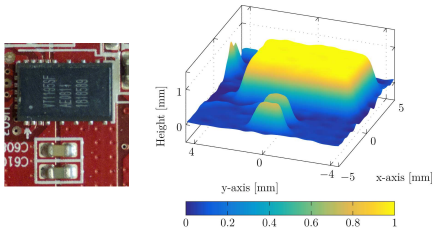

(a) Sample (b) Reconstructed surface profile

Fig. 12. 3D measurement results of the shown (a) voltage regulator on a graphics card. In the reconstructed surface profile (b) not only the regulator but also the SMD resistors are observable.

can be achieved by an integrated mechatronic design in combination with sophisticated motion control. A proper system integration with focus on the target application, utilizing the interplay between process design and control design, allows optimizing the performance of the mechatronic imaging system for the specific application. In this paper such a performance improvement is demonstrated for the example of a FSM in a scanning optical 3D metrology system. By tailoring feedback controllers to the properties of a pre-defined Lissajous trajectory, the tracking error can be reduced by one order of magnitude as compared to the conventional combination of a raster trajectory and a PID controller. Considering also the FSM dynamics and tuning the axis resonances to the reference frequencies, the current consumption can be reduced by a factor of 10 compared to a conventional FSM. Vice-versa the scan area of the tuned FSM is increased by a factor of 60. The final integration of the FSM, a laser triangulation sensor, and the real-time control and data acquisition system demonstrates that a high precision 3D metrology system can be obtained.

Acknowledgements

The financial support by the Austrian Federal Ministry for Digital, Business and Enterprise, and the National Foundation for Research, Technology and Development, as well as MICRO-EPSILON MESSTECHNIK GmbH & Co. KG and ATENSOR Engineering and Technology Systems is gratefully acknowledged.

References

(1) P. Hansma, G. Schitter, G. Fantner, and C. Prater, "High speed atomic force microscopy," *Science*, vol. 314, pp. 601–602, 2006.
(2) H. Butler, "Position control in lithographic equipment," *IEEE Control Systems Magazine*, vol. 31, no. 5, 2011.
(3) R. K. Tyson, *Principles of adaptive optics*. CRC press, 2015.
(4) H. W. Yoo, S. Ito, and G. Schitter, "High speed laser scanning mircoscopy by iterative learning control of a galvanometer scanner," *Control Engineering Practice*, vol. 50, pp. 12–21, 2016.
(5) S. Arunkarthick, M. M. Bijeesh, A. S. Vetcha, N. Rastogi, P. Nandakumar, and G. K. Varier, "Design and construction of a confocal laser scanning microscope for biomolecular imaging," *Current Science*, vol. 107, no. 12, pp. 1965–1969, 2014.
(6) G. Schitter, P. J. Thurner, and P. K. Hansma, "Design and input-shaping control of a novel scanner for high-speed atomic force microscopy," *Mechatronics*, vol. 18, no. 5, pp. 282–288, 2008.
(7) S. Kuiper and G. Schitter, "Model-based feedback controller design for dual actuated atomic force microscopy," *Mechatronics*, vol. 22, no. 3, pp. 327–337, 2012.
(8) E. Csencsics and G. Schitter, "System design and control of a resonant fast steering mirror for lissajous-based scanning," *IEEE Transactions on Mechatronics*, vol. 22, no. 5, pp. 1963–1972, 2017.
(9) R. Munnig Schmidt, G. Schitter, A. Rankers, and J. van Eijk, *The Design of High Performance Mechatronics*, 2nd ed. Delft University Press, 2014.
(10) G. Schitter, K. J. Astrom, B. E. DeMartini, P. J. Thurner, K. L. Turner, and P. K. Hansma, "Design and modeling of a high-speed afm-scanner," *IEEE Transactions on Control Systems Technology*, vol. 15, no. 5, pp. 906–915, 2007.
(11) G. Schitter, A. Stemmer, and F. Allgwer, "Robust two-degree-of-freedom control of an atomic force microscope," *Asian Journal of Control*, vol. 6, no. 2, pp. 156–163, 2004.
(12) H. Yoo, M. E. van Royen, W. A. van Cappellen, A. B. Houtsmuller, M. Verhaegen, and G. Schitter, "Automated spherical aberration correction in scanning confocal microscopy," *Review of Scientific Instruments*, vol. 85, p. 123706, 2014.
(13) K. Harding, *Handbook of Optical Dimensional Metrology*. Taylor & Francis, 2013.
(14) F.-A. Vision, *Marktstudie 3-D-Messtechnik in der deutschen Automobil- und Zulieferindustrie*. Fraunhofer Verlag, Stuttgart, 2009.
(15) J. Salzberger, "Optisch, berührungslos, präzise - Optische Messtechnik für die Qualitätssicherung im Prozess," *Laser + Photonik*, vol. 4, pp. 50–53, 2013.
(16) J. Schlarp, E. Csencsics, and G. Schitter, "Optical scanning of a laser sensor for 3d imaging," *IEEE Transactions on Instrumentation and Measurement, submitted*, 2018.
(17) M. Steinbuch, S. Weiland, and T. Singh, "Design of noise and period-time robust high-order repetitive control, with application to optical storage," *Automatica*, vol. 43, no. 12, pp. 2086–2095, 2007.
(18) K. K. Leang and S. Devasia, "Design of hysteresis-compensating iterative learning control for piezo-positioners: Application to atomic force microscopes," *Mechatronics*, vol. 16, no. 3-4, pp. 141–158, 2006.
(19) M. Rioux, "Laser range finder based on synchronized scanners," *Applied Optics*, vol. 23, no. 21, pp. 3837–3844, 1984.
(20) K. Noda, N. Binh-Khiem, Y. Takei, T. Takahata, K. Matsumoto, and I. Shimoyama, "Multi-axial confocal distance sensor using varifocal liquid lens," in *17th International Conference on Solid-State Sensors, Actuators and Microsystems*, Barcelona, 2013, pp. 1499–1502.
(21) P. GmbH. (2017, Mai) Perceptron Helix. [Online]. Available: https://perceptron.com/helix-sensor/
(22) A. J. Pinkerton, "Lasers in additive manufacturing," *Optics & Laser Technology*, vol. 78, pp. 25–32, 2016.
(23) W. Huang and R. Kovacevic, "A laser-based vision system for weld quality inspection," *Sensors*, vol. 11, no. 12, pp. 506–521, 2011.
(24) E. Csencsics, R. Saathof, and G. Schitter, "Design of a dual-tone controller for lissajous-based scanning of fast steering mirrors," *2016 American Control Conference, Boston, MA, USA*, 2016.
(25) L. R. Hedding and R. A. Lewis, "Fast steering mirror design and performance for stabilization and single axis scanning," *SPIE Vol. 1304 Acquisition, Tracking and Pointing IV*, pp. 14–24, 1990.
(26) S. Xiang, S. Chen, X. Wu, D. Xiao, and X. Zheng, "Study on fast linear scanning for a new laser scanner," *Optics & Laser Technology*, vol. 42, no. 1, pp. 42–46, Feb 2010.
(27) A. J. Fleming and A. G. Wills, "Optimal periodic trajectories for band-limited systems," *IEEE Transactions on Control Systems Technology*, vol. 17, no. 3, p. 552, 2009.
(28) M. Sweeney, G. Rynkowski, M. Ketabchi, and R. Crowley, "Design considerations for fast steering mirrors (fsms)," *Optical Scanning 2002, Proceedings of SPIE*, vol. 4773, 2002.

Post-print version of the article: Ernst Csencsics, Shingo Ito, Johannes Schlarp and Georg Schitter, "System Integration and Control of Mechatronic Imaging Systems," *the 4th IEEJ International Workshop on Sensing, Actuation, Motion Control, and Optimization* , Tokio, Japan, 2018.

(29) T. Tuma, J. Lygeros, V. Kartik, A. Sebastian, and A. Pantazi, "High-speed multiresolution scanning probe microscopy based on lissajous scan trajectories," *Nanotechnology*, vol. 23, no. 18, p. 185501, 2012.

(30) T. Tuma, J. Lygeros, A. Sebastian, and A. Pantazi, "Optimal scan trajectories for high-speed scanning probe microscopy," *2012 American Control Conference*, 2012.

(31) D. J. Kluk, M. T. Boulet, and D. L. Trumper, "A high-bandwidth, high-precision, two-axis steering mirror with moving iron actuator," *Mechatronics*, vol. 22, no. 3, pp. 257–270, Apr 2012.

(32) E. Csencsics and G. Schitter, "Parametric pid controller tuning for a fast steering mirror," *1st IEEE Conference on Control Technology and Applications, Kohala Coast, Hawaii, USA*, 2017.

(33) S. Ito, J. Steininger, and G. Schitter, "Low-stiffness dual stage actuator for long rage positioning with nanometer resolution," *Mechatronics*, vol. 29, 2015.

(34) E. Csencsics, "Integrated design of high performance mechatronics for optical inline metrology systems," Ph.D. dissertation, Technische Universität Wien, Vienna, Austria, 2017.

(35) S. Skogestad and I. Postlethwaite, *Multivariable Feedback Control*. John Wiley, New York, 2005.

(36) M. Hafez and T. C. Sidler, "Fast steering two-axis tilt mirror for laser pointing and scanning," *SPIE Vol. 3834*, September 1999.

(37) F. Tarsha-Kurdi, T. Landes, and P. Grussenmeyer, "Hough-transform and extended ransac algorithms for automatic detection of 3d building roof planes from lidar data," *ISPRS Workshop on Laser Scanning 2007 and SilviLaser 2007*, 2007.

(38) J. Schlarp, E. Csencsics, and G. Schitter, "Feature detection and scan area selection for 3d laser scanning sensors," *IEEE/ASME International Conference on Advanced Intelligent Mechatronic, submitted*, 2018.

Post-print version of the article: Ernst Csencsics, Shingo Ito, Johannes Schlarp and Georg Schitter, "System Integration and Control of Mechatronic Imaging Systems," *the 4th IEEJ International Workshop on Sensing, Actuation, Motion Control, and Optimization* , Tokio, Japan, 2018.